CDDpress

www.nature.com/cdd

ARTICLE

Check for updates

ENKD1 promotes epidermal stratification by regulating spindle orientation in basal keratinocytes

Tao Zhong[1,3], Xiaofan Wu[2,3], Wei Xie[1], Xiangrui Luo[1], Ting Song[1], Shuang Sun[1], Youguang Luo[1], Dengwen Li[2], Min Liu[1], Songbo Xie[1]✉ and Jun Zhou[1,2]✉

Stratification of the epidermis is essential for the barrier function of the skin. However, the molecular mechanisms governing epidermal stratification are not fully understood. Herein, we demonstrate that enkurin domain-containing protein 1 (ENKD1) contributes to epidermal stratification by modulating the cell-division orientation of basal keratinocytes. The epidermis of *Enkd1* knockout mice is thinner than that of wild-type mice due to reduced generation of suprabasal cells from basal keratinocytes through asymmetric division. Depletion of ENKD1 impairs proper orientation of the mitotic spindle and delays mitotic progression in cultured cells. Mechanistic investigation further reveals that ENKD1 is a novel microtubule-binding protein that promotes the stability of astral microtubules. Introduction of the microtubule-binding domain of ENKD1 can largely rescue the spindle orientation defects in ENKD1-depleted cells. These findings establish ENKD1 as a critical regulator of astral microtubule stability and spindle orientation that stimulates epidermal stratification in mammalian cells.

Cell Death & Differentiation (2022) 29:1719–1729; https://doi.org/10.1038/s41418-022-00958-5

INTRODUCTION

The stratified regenerative epithelium forming the epidermis functions as the first barrier to prevent the body from pathogens and water loss [1]. Epidermal dysfunction is implicated in various skin diseases including xerosis, ichthyosis, atopic dermatitis, and psoriasis [2–5]. The stratified epidermis is formed of several cell layers, where keratinocytes in the basal layer exit from the cell cycle, differentiate, and move upward to form more superficial strata during epidermal development [6, 7]. In addition, during skin wound healing, basal keratinocytes are activated and initiate proliferation, differentiation and migration for epidermal remodeling and proper epidermal stratification and homeostasis. The balance between proliferation and differentiation of basal keratinocytes is known to play an essential role in epidermal stratification, thus maintaining the barrier function of the epidermis.

There is mounting evidence that proper spindle orientation of basal keratinocytes is critical for the stratification of the epidermis [8–11]. In mice, basal keratinocytes divide symmetrically to generate stem-like proliferative epidermal cells at embryonic day 8.5 (E8.5), and the spindle orientation shifts from parallel to perpendicular to the basement membrane at around E13.5, contributing to asymmetric division and the generation of terminally differentiated suprabasal cells [12]. Despite clear knowledge about the timeline of epidermal stratification, the underlying molecular mechanisms of epidermal stratification and homeostasis remain not fully understood.

Precise spatiotemporal regulation of astral microtubules is essential for asymmetric cell division, and many microtubule-binding proteins are involved in this process [13–15]. For example, crotonylation of end-binding protein 1 (EB1), a microtubule plus-end tracking protein, promotes the dynamic interaction between astral microtubules and the leucine-glycine-asparagine (LGN)-nuclear mitotic apparatus (NuMA) complex at the cell cortex, thereby accurately controlling spindle orientation [16]. A systematic analysis of the subcellular distribution of human proteins identified enkurin domain-containing protein 1 (ENKD1, previously known as C16orf48) as a potential microtubule-binding protein [17]. However, the precise structure and function of this protein remain unknown. In this study, we present the first evidence that ENKD1 controls epidermal stratification through its actions on astral microtubules and spindle orientation in basal keratinocytes.

RESULTS

ENKD1 is critical for asymmetric division of basal keratinocytes during epidermal development

In an effort to uncover novel regulators of epidermal stratification, we identified ENKD1 as a protein significantly changed during mouse embryonic epidermal development. To investigate the involvement of ENKD1 in epidermal development, we generated *Enkd1* knockout mice with the *Enkd1* deletion under the control of the *Ubc-ERT2* promoter, which is expressed in a wide variety of tissues (Fig. S1). Tamoxifen-induced excision of *Enkd1* was confirmed (Fig. 1A). To assess the function of the skin barrier, toluidine blue was applied from the outside to investigate if the dye can penetrate into the epidermis [18]. Strikingly, whole-body

[1]College of Life Sciences, Shandong Provincial Key Laboratory of Animal Resistance Biology, Collaborative Innovation Center of Cell Biology in Universities of Shandong, Institute of Biomedical Sciences, Shandong Normal University, Jinan 250014, China. [2]College of Life Sciences, State Key Laboratory of Medicinal Chemical Biology, Haihe Laboratory of Cell Ecology, Nankai University, Tianjin 300071, China. [3]These authors contributed equally: Tao Zhong, Xiaofan Wu. ✉email: xiesongbo@sdnu.edu.cn; junzhou@sdnu.edu.cn

Edited by M Hardwick

Received: 2 September 2021 Revised: 8 February 2022 Accepted: 9 February 2022
Published online: 23 February 2022

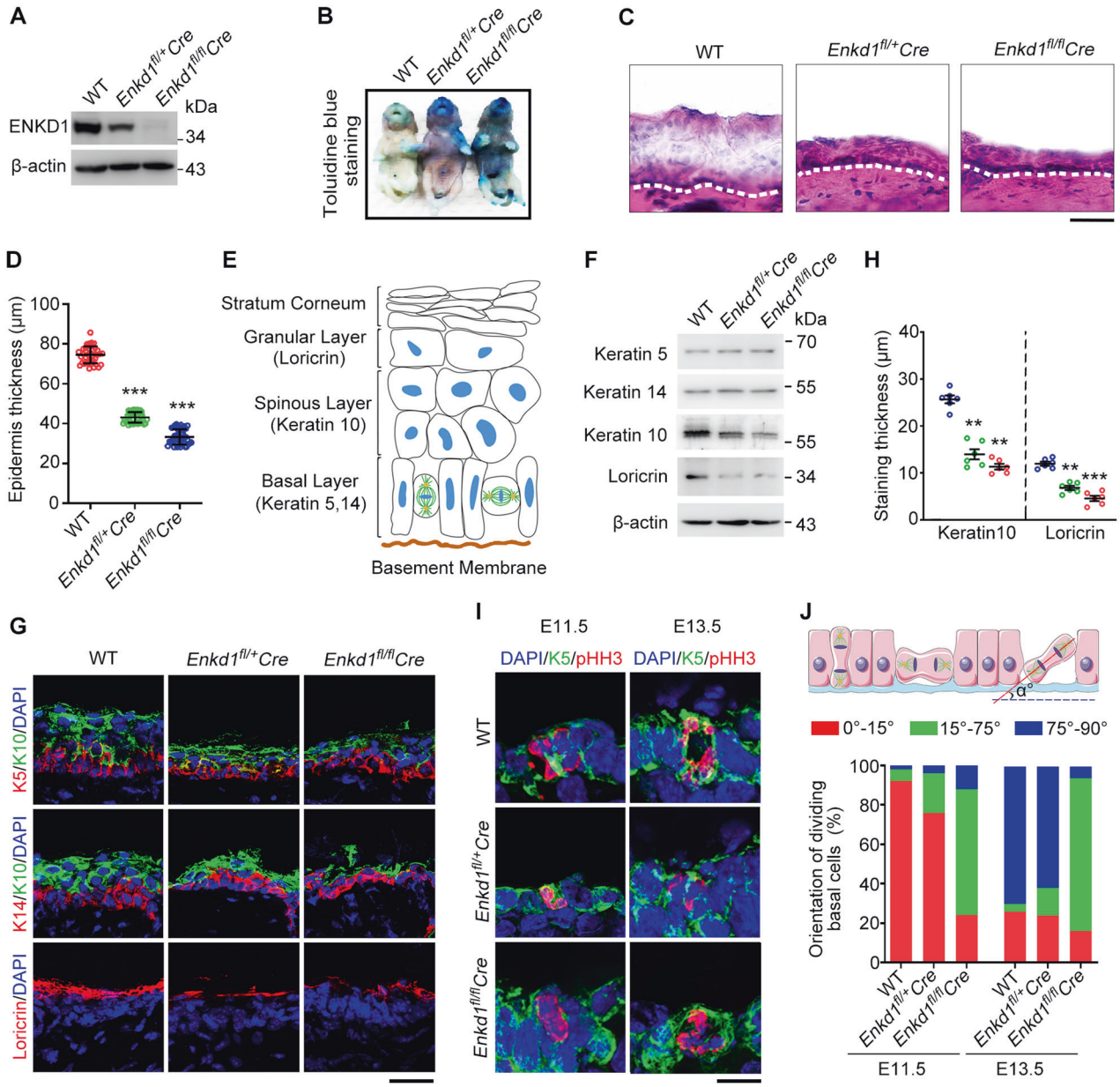

Fig. 1 ENKD1 is essential for epidermal development. **A** Immunoblot analysis of ENKD1 in mouse skin after tamoxifen treatment. **B** Representative images of newborn mice stained with toluidine blue. **C** Hematoxylin and eosin staining of the epidermis of newborn mice. Dashed lines represent the dividing line between dermis and epidermis. Scale bar, 40 μm. **D** Quantification of the thickness of dorsal epidermis. **E** Schematic showing the epidermal layers and their markers. **F** Immunoblot analysis of the indicated markers in the epidermis. **G** Representative images of the epidermis from newborn mice stained with the indicated markers. Scale bar, 30 μm. **H** Quantification of the thickness of keratin 10 (K10)- and loricrin-positive layers. **I** Representative images of the epidermis from E11.5 and E13.5 mice stained with anti-keratin 5 (K5) and anti-phospho-histone H3 (pHH3) antibodies and DAPI. Scale bar, 10 μm. **J** Quantification of the spindle angle of basal keratinocytes as in **I**. $^{**}P < 0.01$; $^{***}P < 0.001$.

penetration of toluidine blue was observed in newborn heterozygous (*Enkd1*$^{fl/+}$*Cre*) and homozygous (*Enkd1*$^{fl/fl}$*Cre*) mice while the skin of wild-type (WT) mice was nearly impermeable to the dye (Fig. 1B), suggesting that the barrier function of epidermis is severely impaired by ENKD1 depletion. Moreover, hematoxylin and eosin (HE) staining revealed a thinner epidermis of *Enkd1* knockout mice compared with that of WT mice (Fig. 1C, D), which is consistent with the severe barrier defect of epidermis in *Enkd1* knockout mice.

The epidermis is composed of the stratum corneum, granular, spinous, and basal layers (Fig. 1E). We next examined which layers were affected by ENKD1 depletion. Immunoblotting revealed that ENKD1 depletion decreased the levels of keratin 10 (a spinous cell marker) and loricrin (a granular cell marker) without affecting keratin 5 and keratin 14 (basal cell markers) (Fig. 1F), suggesting a decrease in granular and spinous layers. We investigated this possibility by immunostaining the epidermis from newborn mice. We observed a significant reduction in the thickness of granular and spinous layers in both *Enkd1*$^{fl/+}$*Cre* and *Enkd1*$^{fl/fl}$*Cre* mice (Fig. 1G, H).

Since the granular and spinous layers consist of post-mitotic suprabasal keratinocytes derived from basal keratinocytes through asymmetric division [19], it is possible that the decrease in granular and spinous layers is due to a defect in asymmetric

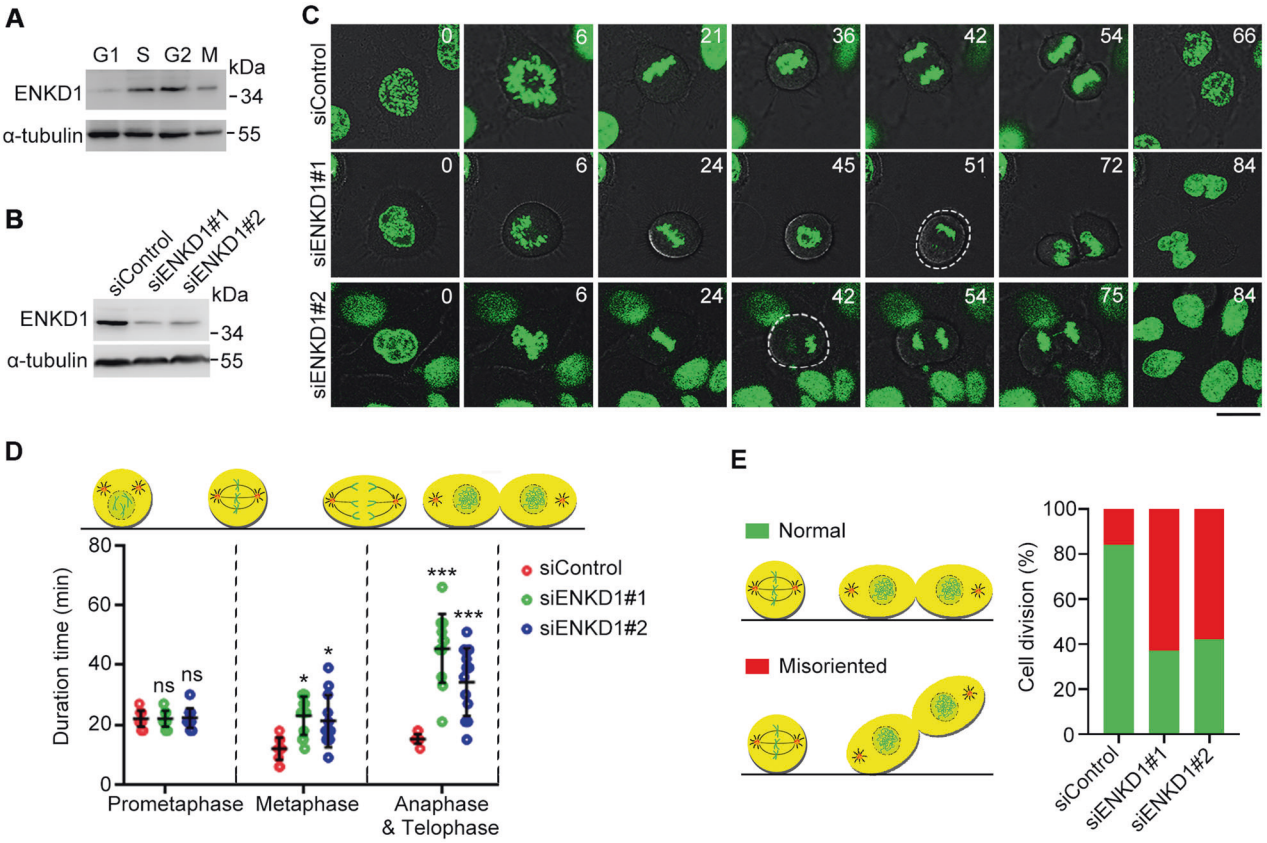

Fig. 2 ENKD1 depletion delays mitotic progression and causes cell-division misorientation. A Immunoblot analysis of the level of ENKD1 in different cell cycle stages. **B** Immunoblot analysis of the knockdown efficacy of ENKD1 siRNAs in HeLa-H2B cells. **C** Time-lapse images showing delayed mitotic progression and uneven timing of daughter cell adhesion to the substratum in siENKD1-treated HeLa-H2B cells compared with control. Dashed lines indicate daughter cells that are not in the same focal plane. Scale bar, 20 μm. Quantification of the duration of mitotic phases (**D**) and misoriented cell division (**E**) in cells treated as in **C**. ns not significant; $^{*}P < 0.05$; $^{***}P < 0.001$.

division of basal keratinocytes. To test this possibility, we examined the cell-division orientation of basal keratinocytes. In WT mice, the basal keratinocytes divided symmetrically with an orientation parallel to the basement membrane at E11.5, and the cell-division orientation changed to perpendicular at E13.5 (Fig. 1I, J). In contrast, in *Enkd* $^{fl/fl}$*Cre* mice, at E11.5 and E13.5, the majority of basal keratinocytes divided at an angle between 15° and 75°, indicative of misoriented division of basal keratinocytes (Fig. 1I, J). These data suggest that ENKD1 plays a vital role in facilitating oriented division of basal keratinocytes.

Loss of ENKD1 leads to misoriented cell division and inhibits cell proliferation

To analyze the role of ENKD1 in mitotic progression, we first examined its level in different cell cycle stages. We found that ENKD1 was highly expressed in S, G2, and M phases (Fig. 2A), indicating a potential role for this protein in mitotic progression. We then knocked down ENKD1 (Fig. 2B) and performed time-lapse imaging to record the mitotic progression of HeLa cells stably expressing GFP-tagged histone 2B (Fig. 2C). ENKD1 deficiency delayed mitotic progression due to the prolonged metaphase and anaphase/telophase (Fig. 2C, D). Strikingly, ENKD1 depletion increased misoriented cell division, in which daughter cells adhered to the substratum with uneven timing (Fig. 2C, E). Taken together, these results indicate a critical role for ENKD1 in oriented cell division.

To further dissect how ENKD1 depletion impairs epidermal stratification, we investigated the in vivo function of ENKD1 in cell proliferation and apoptosis. Immunofluorescence staining with two cell proliferation markers, EdU and phospho-histone H3 (pHH3), demonstrated that the proliferation rate of basal keratinocytes and suprabasal cells was significantly reduced in both *Enkd1*$^{fl/+}$*Cre* and *Enkd1*$^{fl/fl}$*Cre* mice (Fig. S2A, B), whereas there was no obvious difference in the occurrence of apoptosis in basal keratinocytes and suprabasal cells of these mice (Fig. S2C, D). Consistently, immunoblotting revealed that ENKD1 deficiency led to a decrease in the levels of cell proliferation markers such as Ki67, proliferating cell nuclear antigen (PCNA), and pHH3, but did not affect the levels of apoptosis markers such as B-cell CLL/lymphoma 2 (BCL-2), BCL-2 associated X protein (BAX), caspase 3, and cleaved caspase 3 (CC-3) (Fig. S2E). We then sought to verify the effects of ENKD1 on cell proliferation and apoptosis using cultured HaCaT human skin keratinocytes. Consistent with the in vivo findings, knockdown of ENKD1 suppressed the proliferation of HaCaT cells (Fig. S3A, B, E), but did not significantly affect the rate of apoptosis in these cells (Fig. S3C–E).

ENKD1 is essential for spindle orientation in keratinocytes

To explore the cellular mechanisms leading to impaired epidermal development in *Enkd1* knockout mice, we analyzed changes in spindle orientation in HaCaT keratinocytes. The knockdown efficacy of ENKD1 siRNAs in these cells was confirmed by immunoblotting (Fig. 3A). To confirm the role of ENKD1 in spindle orientation, we measured the angle between the spindle axis and the substratum (Fig. 3B). Time-lapse microscopy revealed that the spindle orientation in ENKD1-depleted cells was dramatically altered compared to the control group (Fig. 3C, D). Although the spindle length was not affected (Fig. 3E, F), the average spindle angle was significantly increased (Fig. 3E, G) and the spindle angle distribution was wider in ENKD1-depleted cells (Fig. 3E, H),

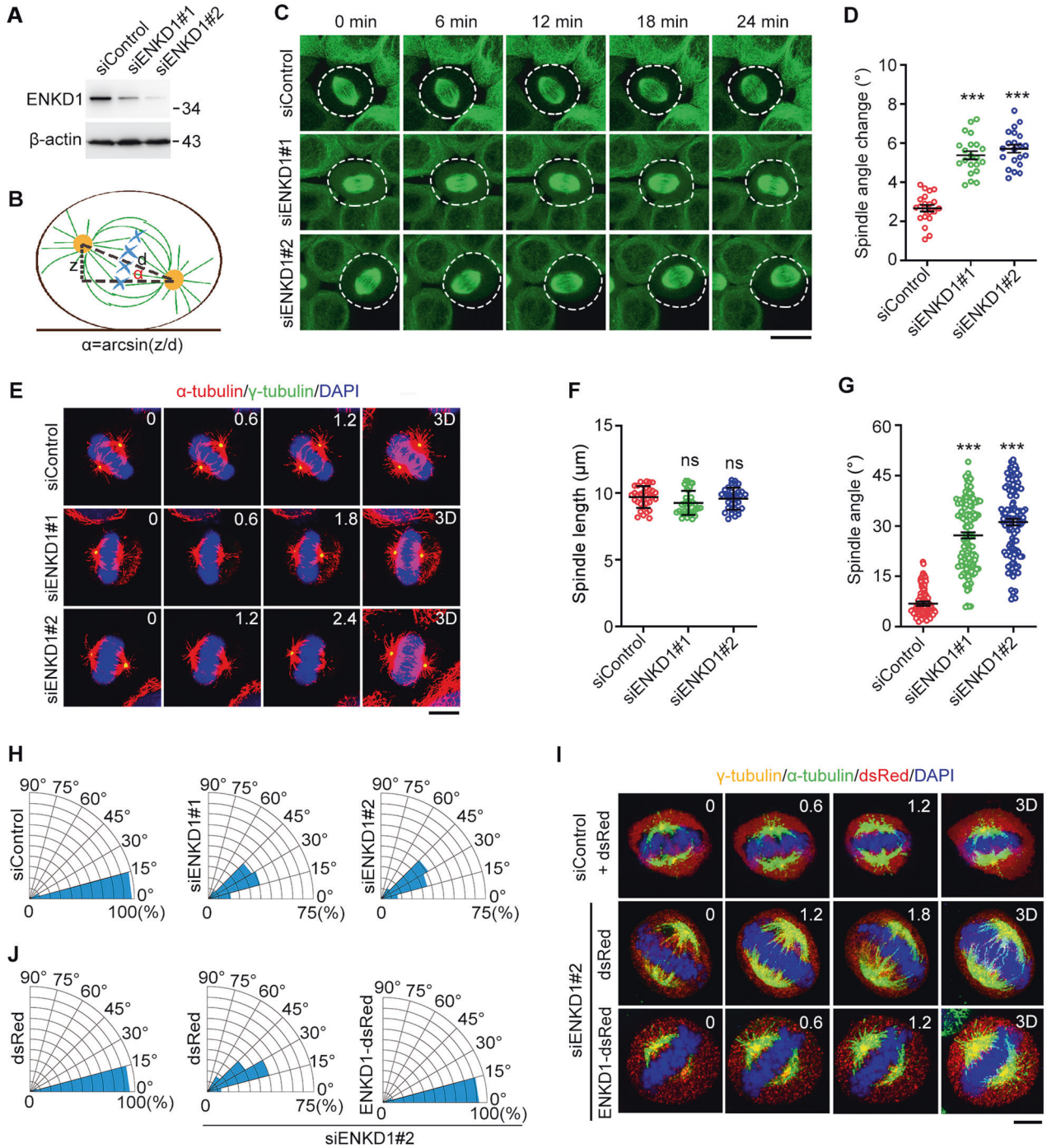

Fig. 3 Loss of ENKD1 leads to spindle orientation defects. A Immunoblots showing the efficacy of ENKD1 siRNAs in HaCaT keratinocytes. **B** Schematic depicting the measurement of the spindle angle (α). **C** Time-lapse images of mitotic cells transfected with GFP-α-tubulin and control or ENKD1 siRNAs. Scale bar, 15 μm. **D** Quantification of changes in spindle orientation in cells treated as in **C**. Representative immunofluorescence images (**E**), spindle length (**F**), spindle angle (**G**), and spindle angle distribution (**H**) of metaphase HaCaT cells transfected with control or ENKD1 siRNAs and stained with anti-α-tubulin (red) and anti-γ-tubulin (green) antibodies and DAPI (blue). The position of the z stage is indicated in micrometers; 3D, x-y projection. Scale bar, 10 μm. Representative immunofluorescence images (**I**) and spindle angle distribution (**J**) of metaphase HaCaT cells transfected with ENKD1 siRNA and dsRed or ENKD1-dsRed followed by staining with anti-α-tubulin (green) and anti-γ-tubulin (yellow) antibodies and DAPI (blue). Scale bar, 10 μm. ns not significant; ***$P < 0.001$.

indicative of spindle misorientation. To confirm the specific role for ENKD1 in spindle orientation, we overexpressed ENKD1-dsRed in ENKD1-depleted cells and found that reintroduction of ENKD1 rescued siENKD1-induced spindle misorientation (Fig. 3I, J). These data indicate that ENKD1 is essential for spindle orientation in keratinocytes.

ENKD1 promotes the stability of astral microtubules in mitotic cells

Numerous studies have demonstrated that the interaction between astral microtubules and the cell cortex dictates spindle orientation [15, 20, 21]. Thus, we examined the effect of ENKD1 on astral microtubule stability. Immunostaining of mitotic cells

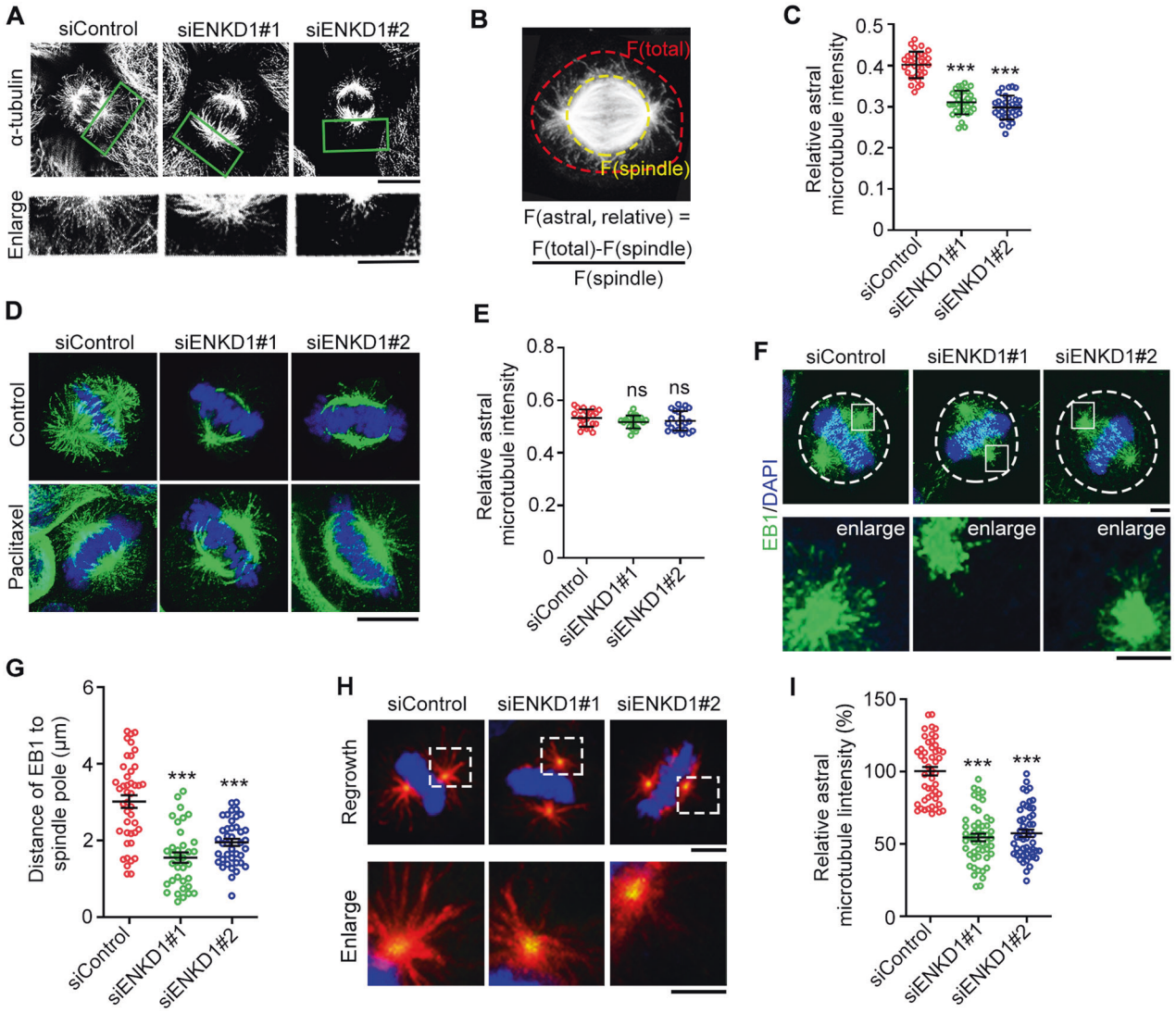

Fig. 4 ENKD1 enhances the stability of astral microtubules in mitotic cells. A Immunofluorescence images of metaphase HaCaT cells stained with anti-α-tubulin antibodies. Scale bars, 10 μm (upper panel) and 5 μm (lower panel). **B** Schematic for the measurement of relative astral microtubule intensity. **C** Quantification of relative astral microtubule intensity in cells treated as in **A**. **D** Immunofluorescence images of metaphase HaCaT cells treated with control or paclitaxel and stained with anti-α-tubulin antibodies. Scale bar, 10 μm. **E** Quantification of relative astral microtubule intensity in cells treated as in **D**. **F** Immunofluorescence images of metaphase HaCaT cells transfected with control or ENKD1 siRNAs and stained with anti-EB1 antibodies and DAPI. Dashed white lines outline cell boundaries. Scale bars, 4 μm. **G** Quantification of the distance between EB1 comets and spindle poles in cells treated as in **F**. **H** Immunofluorescence images of metaphase HaCaT cells treated on ice for 30 min to induce astral microtubule disassembly and then incubated at 37 °C to allow astral microtubule regrowth, followed by staining with anti-α-tubulin antibodies. Scale bars, 8 μm. **I** Quantification of astral microtubule intensity in cells treated as in **H**. ns not significant; ***$P < 0.001$.

revealed that ENKD1 depletion reduced astral microtubules by approximately 20% compared with control (Fig. 4A–C). Importantly, the impaired astral microtubules caused by ENKD1 depletion could be rescued by the microtubule stabilizing agent paclitaxel (Fig. 4D, E). The microtubule plus-end tracking protein EB1 plays a critical role in controlling astral microtubule stability during mitosis [22, 23]. We found that ENKD1 depletion markedly reduced the distance between EB1 comets and the spindle pole, indicative of shortened astral microtubule length (Fig. 4F, G). Furthermore, we disassembled astral microtubules on ice and then analyzed the role of ENKD1 in astral microtubule regrowth. We found that ENKD1 depletion attenuated the regrowth of astral microtubules (Fig. 4H, I). These findings suggest a critical role for ENKD1 in regulating astral microtubule stability during mitosis.

ENKD1 is crucial for microtubule stability in interphase cells

To gain further insights into the role of ENKD1, we examined its effect on interphase microtubules. Immunofluorescence analysis revealed that ENKD1 deficiency exacerbated ice-induced microtubule depolymerization (Fig. 5A, B). After complete microtubule depolymerization, we incubated cells at 37 °C to induce microtubule regrowth. Consistently, ENKD1 deficiency attenuated microtubule regrowth (Fig. 5C, D). To substantiate the role of ENKD1 in microtubule stability, we overexpressed ENKD1 in HaCaT cells and found that its overexpression induced microtubule bundles resistant to ice-induced microtubule depolymerization (Fig. 5E, F). As acetylated microtubules represent stable microtubules, we thus examined whether ENKD1 affects microtubule acetylation. Both immunoblotting and immunofluorescence microscopy confirmed that ENKD1 knockdown decreased

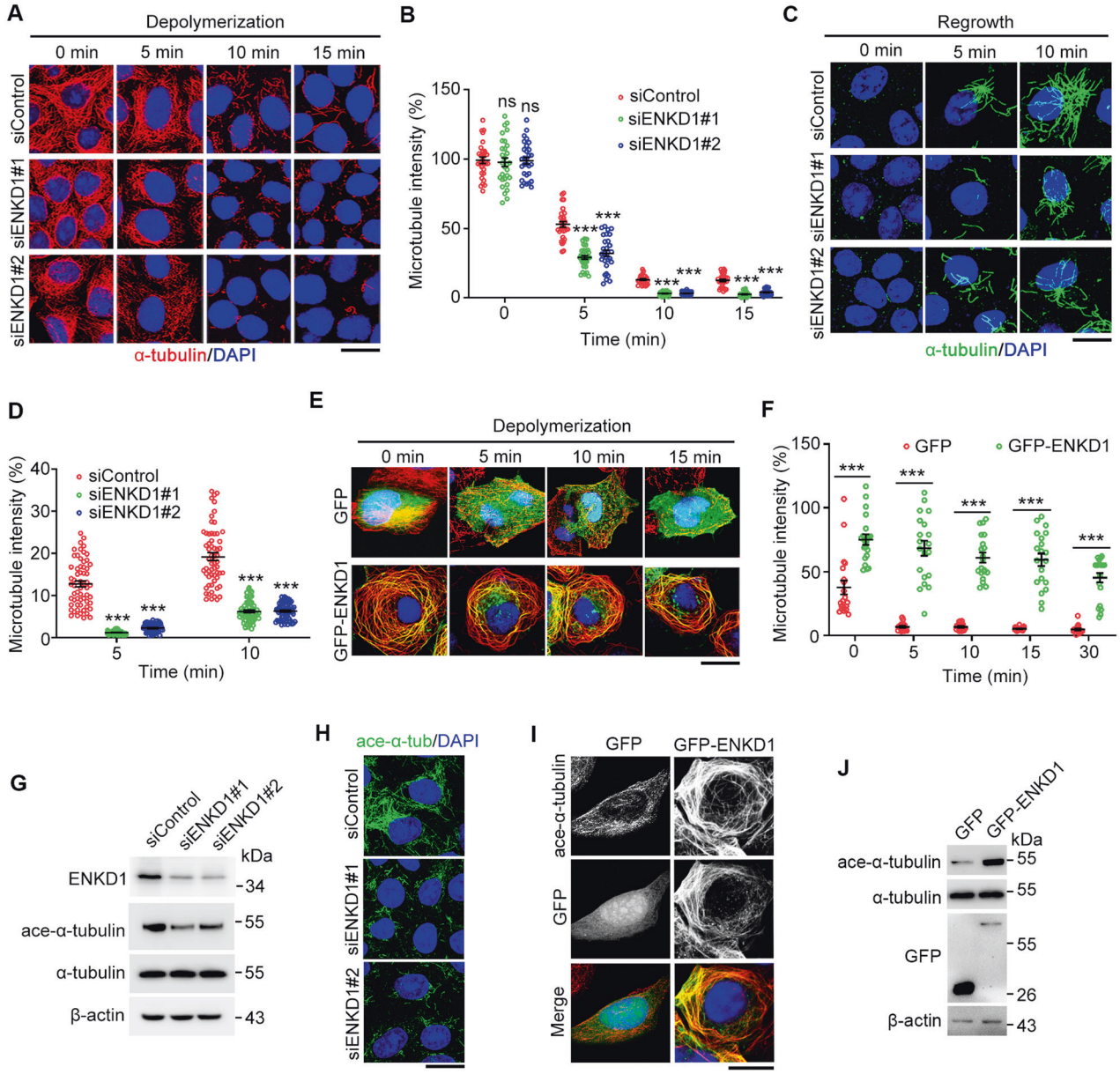

Fig. 5 ENKD1 promotes the stability of interphase microtubules. A Immunofluorescence images of HaCaT cells transfected with control or ENKD1 siRNAs and incubated on ice for the indicated time, followed by staining with anti-α-tubulin antibodies and DAPI. Scale bar, 10 μm. **B** Quantification of microtubule intensity in cells treated as in **A**. **C** Immunostaining with anti-α-tubulin antibodies and DAPI in HaCaT cells transfected with control or ENKD1 siRNAs, followed by incubating on ice for 45 min to induce complete microtubule disassembly and incubation at 37 °C for the indicated time. Scale bar, 10 μm. **D** Quantification of microtubule intensity in cells treated as in **C**. **E** Immunostaining with anti-α-tubulin antibodies and DAPI in HaCaT cells transfected with GFP or GFP-ENKD1, followed by incubation on ice for the indicated time. Scale bar, 10 μm. **F** Quantification of microtubule intensity in cells treated as in **E**. **G** Immunoblots showing levels of ENKD1, acetylated α-tubulin, α-tubulin, and β-actin in HaCaT cells transfected with control or ENKD1 siRNAs. **H** Immunostaining with anti-acetylated α-tubulin antibodies and DAPI in HaCaT cells transfected with control or ENKD1 siRNAs. Scale bar, 10 μm. **I** Immunostaining with anti-acetylated α-tubulin antibodies and DAPI in HaCaT cells transfected with GFP or GFP-ENKD1. Scale bar, 10 μm. **J** Immunoblotting with anti-acetylated α-tubulin, α-tubulin, GFP, and β-actin antibodies in HaCaT cells transfected with GFP or GFP-ENKD1. ns not significant; ***$P < 0.001$.

microtubule acetylation (Fig. 5G, H) and, conversely, ENKD1 overexpression promoted microtubule acetylation (Fig. 5I, J). Collectively, these data indicate that ENKD1 play a crucial role in regulating microtubule stability.

ENKD1 is a novel microtubule-binding protein that interacts with microtubules via the 91-171 amino acid region

We next investigated whether ENKD1 regulates microtubule stability directly. Immunofluorescence analysis demonstrated that GFP-ENKD1 co-localized with both interphase microtubules (Fig. 6A) and mitotic spindle microtubules (Fig. 6B). To examine whether ENKD1 is a novel microtubule-binding protein, we performed immunoprecipitation experiments. We found that both GFP-tagged and GST-tagged ENKD1 interacted with α-tubulin (Fig. 6C, D). Furthermore, microtubule co-sedimentation assays showed that exogenously expressed GFP-ENKD1 was present in microtubule pellets in the presence of paclitaxel and GTP (P/G), whereas GFP was present in supernatants (Fig. 6E). Consistently, endogenous ENKD1 was pelleted along with microtubules (Fig. 6F), indicating an interaction between ENKD1 and microtubules.

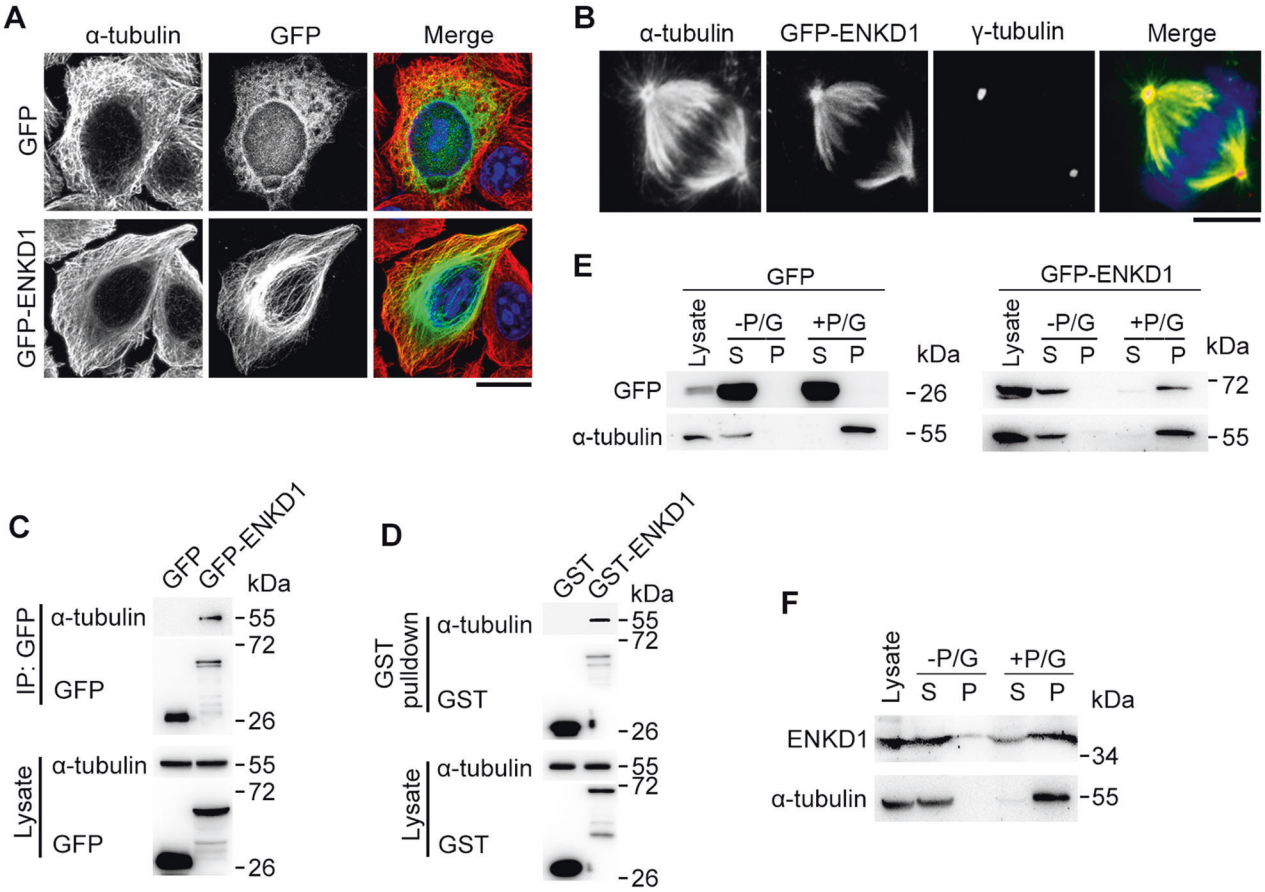

Fig. 6 ENKD1 is a novel microtubule-binding protein. A Immunofluorescence images of HaCaT cells transfected with GFP or GFP-ENKD1 and stained with anti-α-tubulin antibodies and DAPI. Scale bar, 10 μm. **B** Immunostaining with anti-α-tubulin and anti-γ-tubulin antibodies in ENKD1-depleted HaCaT cells transfected with GFP-ENKD1. Scale bar, 6 μm. **C** Immunoprecipitation and immunoblotting showing the interaction between GFP-ENKD1 and α-tubulin. **D** GST pulldown and immunoblotting showing the interaction between GST-ENKD1 and α-tubulin. **E** Microtubule co-sedimentation showing that GFP-ENKD1 was present in microtubule-associated pellets in the presence of paclitaxel and GTP (P/G), whereas GFP was present in the supernatant. **F** Microtubule co-sedimentation showing that endogenous ENKD1 was pelleted by microtubules in the presence of paclitaxel and GTP.

To identify the domains of ENKD1 that mediate its interaction with microtubules, we constructed a series of GFP-tagged ENKD1 truncations (Fig. 7A). Immunofluorescence microscopy revealed that the 91-250 amino acid (aa) region was required for the co-localization of ENKD1 with microtubules (Fig. 7B). Immunoprecipitation further confirmed the requirement of this region for the binding of ENKD1 to microtubules (Fig. 7C). To establish the minimal region in ENKD1 responsible for its binding to microtubules, we split the 91-250 aa region into three fragments: 91-171 aa, 172-210 aa, and 211-250 aa (Fig. 7D), and found that the 91-171 aa region was indispensable for ENKD1 binding to microtubules (Fig. 7E). In addition, we found that deletion of this region abolished the interaction between ENKD1 and microtubules (Fig. 7F). Importantly, full-length ENKD1 and the 91-171 aa region, but not Δ(91-171), rescued the spindle orientation defects caused by ENKD1 depletion (Fig. 7G–I). Taken together, these data indicate that ENKD1 is a novel microtubule-binding protein that regulates spindle orientation via its microtubule-binding activity.

DISCUSSION

The epidermis is the largest tissue of the human body, and it undergoes constant renewal throughout life [24, 25]. Understanding the mechanisms underlying epidermal stratification is important due to the potential to exploit these mechanisms for wound repair, skin transplantation, and treatment of various skin diseases [26–28]. In this study, we have identified a critical role for ENKD1 in epidermal development. Although *Enkd1* knockout mice survive and grow normally, their skin is thinner due to the reduced generation of suprabasal cells, indicating a defect in epidermal stratification. Given the importance of epidermal stratification in maintaining skin barrier function, it is therefore tempting to speculate that *Enkd1* knockout mice may suffer from severe infectious diseases when they are exposed to pathogens. In addition, ENKD1 is essential for the proliferation of basal keratinocytes and suprabasal cells. Consistently, ENKD1 is found to promote the growth of non-small cell lung cancer cells [29], suggesting that the alteration of ENKD1 expression might be implicated in cancer development.

The anchorage of astral microtubules by evolutionarily conserved cortical force generators, such as the NuMA/LGN/Gαi complex, plays a crucial role in spindle orientation [21, 30]. There is emerging evidence that perturbation of astral microtubules leads to spindle misorientation [21, 31]. The present study demonstrates ENKD1 as a novel microtubule-binding protein, with its microtubule-binding activity critical for the regulation of spindle orientation in basal keratinocytes, further supporting the importance of microtubule-binding proteins in spindle orientation. The cylindromatosis (CYLD) tumor suppressor protein, a microtubule-binding deubiquitinase, has been shown to modulate spindle orientation by stabilizing astral microtubules and stimulating dishevelled-NuMA-dynein/dynactin complex formation, thus

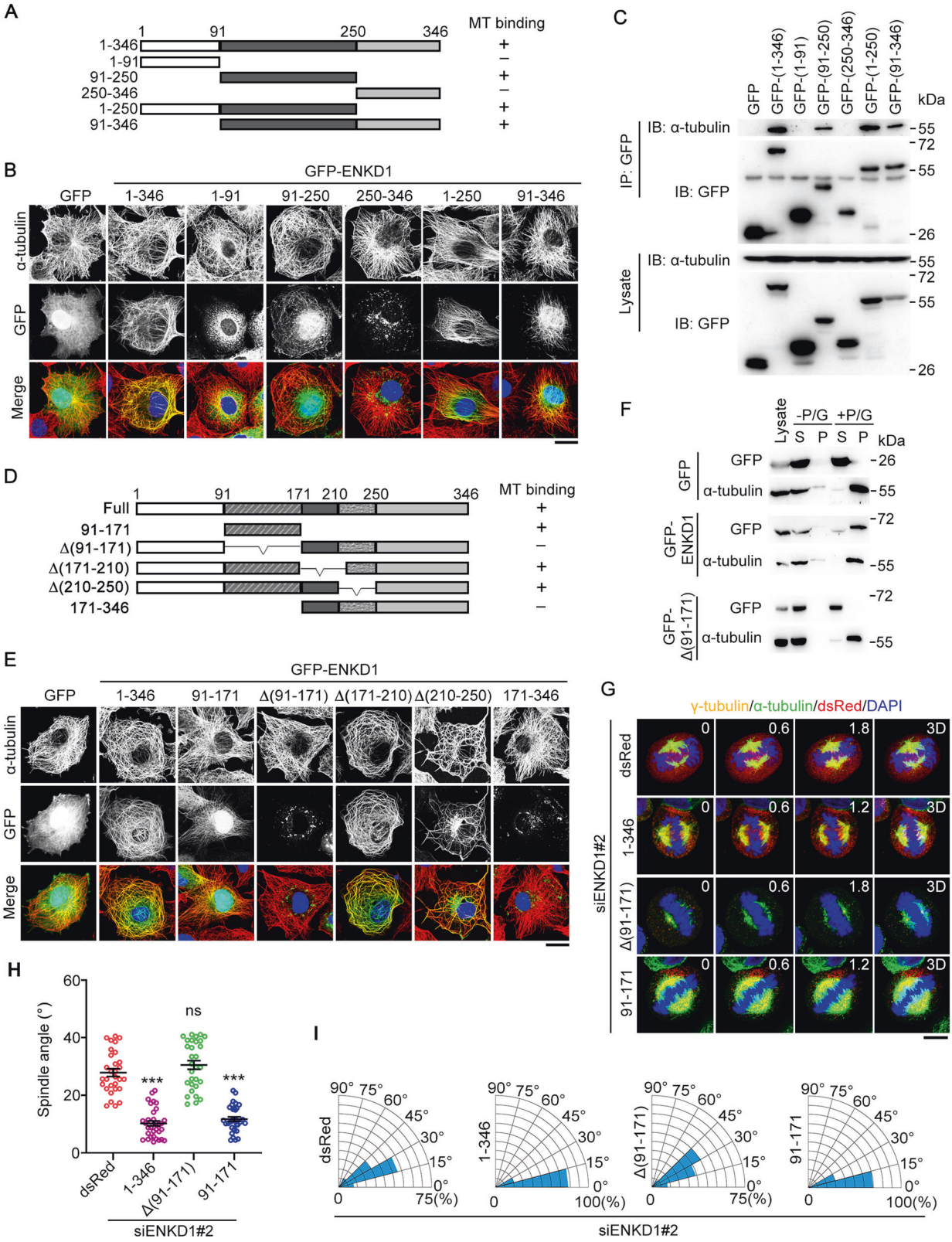

anchoring astral microtubules to the cortical force generators [15]. It will be interesting to examine whether ENKD1 acts as a bridge connecting astral microtubules to the cell cortex.

The present study shows that the 91–171 aa region of ENKD1 is responsible for its interaction with microtubules; however, this region does not contain any conserved microtubule-binding motifs like the cytoskeleton-associated protein-glycine-rich domain [32, 33]. Enkurin, a flagellar protein initially identified as a potential regulator of transient receptor potential (TRP) channels, is essential for sperm motility [34, 35]. ENKD1 contains

Fig. 7 ENKD1 interacts with microtubules via the 91-171 amino acid region. A Schematic showing the microtubule-binding ability of full-length ENKD1 and truncated mutants. **B** Representative images of HaCaT cells transfected with GFP or GFP-ENKD1 plasmids and stained with anti-α-tubulin antibodies. Scale bar, 10 μm. **C** Immunoprecipitation and immunoblotting showing the interaction between GFP-ENKD1 proteins and α-tubulin. **D** Schematic showing the microtubule-binding ability of full-length ENKD1 and truncated mutants. **E** Representative images of HaCaT cells transfected with the indicated plasmids and stained with anti-α-tubulin antibodies. Scale bar, 10 μm. **F** Microtubule co-sedimentation showing that the 91–171 amino acid region of ENKD1 interacted with microtubules. Representative images (**G**), average spindle angle (**H**), and the distribution of the spindle angle (**I**) of ENKD1-depleted HaCaT cells transfected with dsRed, ENKD1-dsRed or its truncated mutants, and stained with anti-α-tubulin (green) and anti-γ-tubulin (yellow) antibodies and DAPI (blue). The position of the z stage is indicated in micrometers; 3D, x-y projection. Scale bar, 6 μm. ns not significant; ***$P < 0.001$.

an enkurin domain (250–343 aa); however, our study reveals that the enkurin domain of ENKD1 does not mediate its interaction with microtubules. As epidermal keratinocytes broadly express many TRP channels [36], it might be important to analyze whether the enkurin domain is involved in the regulation of spindle orientation in basal keratinocytes and epidermal stratification through TRP channel interactions. In addition, a recent study using evolutionary proteomics has identified ENKD1 as a potential ciliary protein [37]. The amino acid sequences of ENKD1 are highly conserved across multiple species (Fig. S4). Given the importance of primary cilia in epidermal development, it will be interesting to investigate in the future whether a ciliary function of ENKD1 synergizes with its microtubule-binding activity to regulate epidermal stratification.

In conclusion, the present study identifies a critical role for ENKD1 in epidermal stratification by modulating the cell-division orientation of basal keratinocytes. In addition, we demonstrate that ENKD1 is a novel microtubule-binding protein and promotes the stability of astral microtubules, thereby facilitating proper orientation of the mitotic spindle. These results, together with previous findings [15], indicate that microtubule-binding proteins may act as important regulators of epidermal stratification. Further studies are warranted to study the structural details of how these proteins regulate microtubule properties and whether their alterations are associated with epidermal diseases.

MATERIALS AND METHODS

Materials

Antibodies targeting ENKD1 (#ab224560), keratin 5 (#ab52635), keratin 10 (#ab9025), pHH3 (#ab10543), α-tubulin (#ab7291), Ki67 (#ab16667), PCNA (#ab92552), caspase 3 (#ab13847), CC-3 (#ab214430), and Alexa Fluor-conjugated secondary antibodies (#ab150081, #ab175694, #ab150117, #ab175699) were purchased from Abcam (Cambridge, UK). Antibodies targeting acetylated α-tubulin (#T7451), γ-tubulin (#T6557, #T3320), GFP (#G1544), GST (#SAB5300159), BAX (#SAB4502546), BCL-2 (#SAB4500003), and β-actin (#A5441) were from Sigma-Aldrich (St Louis, MO, USA). Antibodies targeting keratin 14 (#CY5683, Abways, Shanghai, China), loricrin (#55439-1-AP, ProteinTech, Rosemont, IL, USA), and EB1 (#610534, BD Bioscience, San Jose, CA, USA) were purchased from the indicated sources. Horseradish peroxidase–conjugated secondary antibodies were from Santa Cruz Biotechnology (#sc2004, #sc2005, Santa Cruz, CA, USA). 4',6-diamidino-2-phenylindole (DAPI), tamoxifen, and paclitaxel were obtained from Sigma-Aldrich. Mammalian plasmids expressing ENKD1-dsRed, GFP-ENKD1 and GST-ENKD1 were constructed by inserting the *Enkd1* cDNA into the pDsRed1-N1, pEGFP-C1, and pEBG vectors, respectively. Mammalian plasmids expressing GFP-ENKD1 truncations were constructed by PCR with pEGFP-C1-ENKD1 as a template. Human ENKD1 siRNAs (#1: 5'-GGCCCAAAGUCUUCGUGAA-3'; #2: 5'-GUGGACUU-CAUUCGUCACA-3') were synthesized by RiboBio (Guangzhou, China).

Cell culture

HaCaT, HeLa, and HEK-293T cells were obtained from the American Type Culture Collection. HeLa cells stably expressing GFP-histone 2B (HeLa-H2B) were obtained as described previously [14, 15]. Cells were cultured in DMEM (Thermo Fisher Scientific, Waltham, MA, USA) supplemented with 10% fetal bovine serum. Plasmids were transfected into cells with Lipofectamine 3000 (Thermo Fisher Scientific) and siRNAs were transfected with Lipofectamine RNAimax (Thermo Fisher Scientific). All cell lines were assessed regularly for mycoplasma contamination using a MycoAlert PLUS Mycoplasma Detection Kit (Lonza, Basel, Switzerland).

Animal experiments

Enkd1$^{fl/fl}$ mice were generated via the CRISPR/Cas9 system by creating *loxP* sites flanking exon 3 of the *Enkd1* gene. *Enkd1*$^{fl/fl}$ mice were crossed with *Ubc-Cre/ERT2* mice (The Jackson Laboratories, Bar Harbor, ME, USA) for the generation of tamoxifen-inducible *Enkd1* knockout mice. Experiments were performed according to Guide to the Care and Use of Experimental Animals of Shandong Normal University. Frozen and paraffin-embedded sections of the epidermis from E11.5, E13.5, and newborn WT C57BL/6 mice and *Enkd1* knockout mice were immunostained with the indicated antibodies, and results were assessed by blinded evaluators. Sample sizes were determined according to the standard protocols in the field. No randomization was used to allocate male mice to groups.

Epidermal barrier assays

Newborn mice at postnatal day 1 (P1) were euthanized with CO_2 and washed with methanol. Then the mice were submerged in 0.2% toluidine blue solution for 15 min, followed by washing three times with 90% ethanol and once with distilled water. The epidermal barrier function was then determined by the extent of penetration of toluidine blue through the skin, where blue/purple staining indicates a defective barrier.

Cell proliferation and apoptosis assays

For in vivo Edu staining, P1 newborn mice received a hypodermic injection of EdU. The epidermis was harvested 4 h later, embedded, frozen sectioned, and stained with the Cell-Light Apollo Stain Kit (RiboBio) according to the manufacturer's instructions. For in vitro EdU staining, cells were treated with EdU for 24 h, and then analyzed with the EdU cell proliferation detection kit (RiboBio) according to the manufacturer's instructions. Images were taken with a Leica TCS SP8 confocal microscope (Leica, Wetzlar, Germany). The 3-(4,5)-dimethylthiahiazol-2-y1)-2,5-diphenyl tetrazolium bromide (MTT) calorimetric assay was performed to examine the amount of living cells. To examine apoptosis, cells were stained with the FITC Annexin-V Apoptosis Detection Kit (BD Biosciences) followed by examination with a flow cytometer (BD Biosciences) or stained with terminal deoxynucleotidyl transferase-mediated dUTP nick end labeling (TUNEL) Apoptosis Detection Kit (Abcam) and imaged with the TCS SP8 confocal microscope (Leica).

Fluorescence microscopy

Cells grown on coverslips were fixed with 4% paraformaldehyde, permeabilized with 0.5% Triton X-100, and blocked with 2% bovine serum albumin (BSA). Then, cells were sequentially probed with the primary antibodies, fluorophore-conjugated secondary antibodies, and DAPI. The coverslips were mounted with mounting medium and imaged with the TCS SP8 confocal microscope. The spindle angle was determined as described previously [15]. The distance between EB1 comets and spindle poles was analyzed with the Image J software. For time-lapse microscopy, mitotic progression were recorded with the TCS SP8 confocal microscope equipped with a live-cell chamber as described [38].

Immunoblotting, immunoprecipitation, and GST pulldown

Cells were lysed using cell lysis buffer (Beyotime Biotechnology, Shanghai, China), and cell lysates were mixed with sodium dodecyl sulfate (SDS) sample buffer. Proteins were loaded into 10% SDS-polyacrylamide gel, resolved by electrophoresis, and transferred onto polyvinylidene difluoride membranes (Millipore, Burlington, MA, USA). The membranes were blocked in Tris-buffered saline containing 0.1% Tween 20 and 5% fat-

free milk and sequentially incubated with primary antibodies and horseradish peroxidase-conjugated secondary antibodies. Targeted proteins were visualized with an enhanced chemiluminescence substrate kit (Millipore). For immunoprecipitation and GST pulldown, cell lysates were incubated with anti-GFP agarose beads and glutathione agarose beads overnight at 4 °C, respectively. Immunoprecipitates and pulldown pellets were immunoblotted with the indicated antibodies.

Microtubule co-sedimentation

Microtubule co-sedimentation was performed as described with minor modifications [39]. Briefly, nocodazole-treated cells were collected and extracted with PEM/Triton/protease inhibitor buffer followed by centrifugation at 14,000 × *g* at 4 °C for 30 min. The supernatant was added to an equal volume of PEM buffer supplemented with GTP and paclitaxel, and incubated at 4 °C for 20 min. The samples were overlaid on a cushion of PEM buffer containing 50% sucrose, GTP, and paclitaxel and centrifuged at 30,000 × *g* for 30 min. Proteins present in the supernatant and pellet fractions were analyzed by immunoblotting.

Data plotting and statistical analysis

Prism 8 (Graph Pad) was used for data plotting and statistical analysis. All experiments were repeated independently at least three times, and data are expressed as mean ± standard error of the mean (SEM). Significant difference for each experiment was determined by Student's *t*-test for pairwise comparisons and one-way or two-way analysis of variance (ANOVA) for comparison of multiple groups, as appropriate, using the built-in analysis tools of Prism 8. Normal distribution, variation within each group, and sample independence were assumed to be met. All measurements were taken from distinct samples, and no data were excluded. Sample sizes were determined according to the standard protocols. Asterisks denote *P*-value as follows: $*P < 0.05$; $**P < 0.01$; $***P < 0.001$.

DATA AVAILABILITY

The authors declare that all data supporting the findings of this study are available within the paper in the main text or the Supplementary file.

REFERENCES

1. Koster MI, Roop DR. Mechanisms regulating epithelial stratification. Annu Rev Cell Dev Biol. 2007;23:93–113.
2. Lambrecht BN, Hammad H. The immunology of the allergy epidemic and the hygiene hypothesis. Nat Immunol. 2017;18:1076–83.
3. Botchkarev VA, Flores ER. p53/p63/p73 in the epidermis in health and disease. Cold Spring Harb Perspect Med. 2014;4:a015248.
4. Baum S, Sakka N, Artsi O, Trau H, Barzilai A. Diagnosis and classification of autoimmune blistering diseases. Autoimmun Rev. 2014;13:482–9.
5. Charruyer A, Fong S, Vitcov GG, Sklar S, Tabernik L, Taneja M, et al. Interleukin-17A-dependent asymmetric stem cell divisions are increased in human psoriasis: a mechanism underlying benign hyperproliferation. Stem Cells. 2017;35:2001–7.
6. Veltri A, Lang C, Lien WH. Wnt signaling pathways in skin development and epidermal stem cells. Stem Cells. 2018;36:22–35.
7. Gonzales KAU, Fuchs E. Skin and its regenerative powers: an alliance between stem cells and their niche. Dev Cell. 2017;43:387–401.
8. Miroshnikova YA, Le HQ, Schneider D, Thalheim T, Rubsam M, Bremicker N, et al. Adhesion forces and cortical tension couple cell proliferation and differentiation to drive epidermal stratification. Nat Cell Biol. 2018;20:69–80.
9. Miroshnikova YA, Cohen I, Ezhkova E, Wickstrom SA. Epigenetic gene regulation, chromatin structure, and force-induced chromatin remodelling in epidermal development and homeostasis. Curr Opin Genet Dev. 2019;55:46–51.
10. Williams SE, Beronja S, Pasolli HA, Fuchs E. Asymmetric cell divisions promote Notch-dependent epidermal differentiation. Nature. 2011;470:353–8.
11. Williams SE, Ratliff LA, Postiglione MP, Knoblich JA, Fuchs E. Par3-mInsc and Galphai3 cooperate to promote oriented epidermal cell divisions through LGN. Nat Cell Biol. 2014;16:758–69.
12. Xie W, Zhou J. Regulation of mitotic spindle orientation during epidermal stratification. J Cell Physiol. 2017;232:1634–9.
13. Delgado MK, Cabernard C. Mechanical regulation of cell size, fate, and behavior during asymmetric cell division. Curr Opin Cell Biol. 2020;67:9–16.
14. Luo Y, Ran J, Xie S, Yang Y, Chen J, Li S, et al. ASK1 controls spindle orientation and positioning by phosphorylating EB1 and stabilizing astral microtubules. Cell Discov. 2016;2:16033.
15. Yang Y, Liu M, Li D, Ran J, Gao J, Suo S, et al. CYLD regulates spindle orientation by stabilizing astral microtubules and promoting dishevelled-NuMA-dynein/dynactin complex formation. Proc Natl Acad Sci USA. 2014;111:2158–63.
16. Song X, Yang F, Liu X, Xia P, Yin W, Wang Z, et al. Dynamic crotonylation of EB1 by TIP60 ensures accurate spindle positioning in mitosis. Nat Chem Biol. 2021;17:1314–23.
17. Stadler C, Rexhepaj E, Singan VR, Murphy RF, Pepperkok R, Uhlen M, et al. Immunofluorescence and fluorescent-protein tagging show high correlation for protein localization in mammalian cells. Nat Methods. 2013;10:315–23.
18. Hardman MJ, Sisi P, Banbury DN, Byrne C. Patterned acquisition of skin barrier function during development. Development. 1998;125:1541–52.
19. Sotiropoulou PA, Blanpain C. Development and homeostasis of the skin epidermis. Cold Spring Harb Perspect Biol. 2012;4:a008383.
20. van Leen EV, di Pietro F, Bellaiche Y. Oriented cell divisions in epithelia: from force generation to force anisotropy by tension, shape and vertices. Curr Opin Cell Biol. 2020;62:9–16.
21. di Pietro F, Echard A, Morin X. Regulation of mitotic spindle orientation: an integrated view. EMBO Rep. 2016;17:1106–30.
22. Chen M, Cao Y, Dong D, Zhang Z, Zhang Y, Chen J, et al. Regulation of mitotic spindle orientation by phosphorylation of end binding protein 1. Exp Cell Res. 2019;384:111618.
23. Stout JR, Yount AL, Powers JA, LeBlanc C, Ems-McClung SC, Walczak CE, et al. Kif18B interacts with EB1 and controls astral microtubule length during mitosis. Mol Biol Cell. 2011;22:3070–80.
24. Rognoni E, Watt FM. Skin cell heterogeneity in development, wound healing, and cancer. Trends Cell Biol. 2018;28:709–22.
25. Blanpain C, Fuchs E. Epidermal homeostasis: a balancing act of stem cells in the skin. Nat Rev Mol Cell Biol. 2009;10:207–17.
26. Amini-Nik S, Dolp R, Eylert G, Datu AK, Parousis A, Blakeley C, et al. Stem cells derived from burned skin—The future of burn care. EBioMedicine. 2018;37:509–20.
27. Bauer JW, Koller J, Murauer EM, De Rosa L, Enzo E, Carulli S, et al. Closure of a large chronic wound through transplantation of gene-corrected epidermal stem cells. J Invest Dermatol. 2017;137:778–81.
28. Razmi TM, Kumar R, Rani S, Kumaran SM, Tanwar S, Parsad D. Combination of follicular and epidermal cell suspension as a novel surgical approach in difficult-to-treat vitiligo: a randomized clinical trial. JAMA Dermatol. 2018;154:301–8.
29. Song T, Zhou P, Sun C, He N, Li H, Ran J, *et al*. Enkurin domain containing 1 (ENKD1) regulates the proliferation, migration and invasion of non-small cell lung cancer cells. Asia Pac J Clin Oncol. 2021. https://doi.org/10.1111/ajco.13550.
30. Dimitracopoulos A, Srivastava P, Chaigne A, Win Z, Shlomovitz R, Lancaster OM, et al. Mechanochemical crosstalk produces cell-intrinsic patterning of the cortex to orient the mitotic spindle. Curr Biol. 2020;30:3687–96.
31. Lechler T, Mapelli M. Spindle positioning and its impact on vertebrate tissue architecture and cell fate. Nat Rev Mol Cell Biol. 2021;22:691–708.
32. Yan S, Guo C, Hou G, Zhang H, Lu X, Williams JC, et al. Atomic-resolution structure of the CAP-Gly domain of dynactin on polymeric microtubules determined by magic angle spinning NMR spectroscopy. Proc Natl Acad Sci USA. 2015;112:14611–6.
33. D'Alessandro M, Hnia K, Gache V, Koch C, Gavriilidis C, Rodriguez D, et al. Amphiphysin 2 orchestrates nucleus positioning and shape by linking the nuclear envelope to the actin and microtubule cytoskeleton. Dev Cell. 2015;35:186–98.
34. Sutton KA, Jungnickel MK, Wang Y, Cullen K, Lambert S, Florman HM. Enkurin is a novel calmodulin and TRPC channel binding protein in sperm. Dev Biol. 2004;274:426–35.
35. Jungnickel MK, Sutton KA, Baker MA, Cohen MG, Sanderson MJ, Florman HM. The flagellar protein Enkurin is required for mouse sperm motility and for transport through the female reproductive tract. Biol Reprod. 2018;99:789–97.
36. Denda M, Tsutsumi M. Roles of transient receptor potential proteins (TRPs) in epidermal keratinocytes. Adv Exp Med Biol. 2011;704:847–60.
37. Sigg MA, Menchen T, Lee C, Johnson J, Jungnickel MK, Choksi SP, et al. Evolutionary proteomics uncovers ancient associations of cilia with signaling pathways. Dev Cell. 2017;43:744–62.
38. Gao J, Sun L, Huo L, Liu M, Li D, Zhou J. CYLD regulates angiogenesis by mediating vascular endothelial cell migration. Blood. 2010;115:4130–7.
39. Hergovich A, Lisztwan J, Barry R, Ballschmieter P, Krek W. Regulation of microtubule stability by the von Hippel-Lindau tumour suppressor protein pVHL. Nat Cell Biol. 2003;5:64–70.

ACKNOWLEDGEMENTS

We are grateful to Drs. Huijie Zhao, Xueliang Zhu, and Rutao Cui for discussion. This work was supported by grants from the National Natural Science Foundation of China (31730050, 31871347, 32170829, 32070708, 32000490, and 32000870) and the National Key R&D Program of China (2017YFA0503502 and 2021YFA1101001).

AUTHOR CONTRIBUTIONS

TZ and XW performed experiments and analyzed data; WX, XL, TS, SS, YL, DL and ML performed experiments; SX and JZ supervised the project and wrote the manuscript.

COMPETING INTERESTS

The authors declare no competing interests.

ETHICAL STATEMENT

All applicable institutional and/or national guidelines for the care and use of animals were followed. The use of mice was approved by the Animal Care and Use Committee of Shandong Normal University.

ADDITIONAL INFORMATION

Supplementary information The online version contains supplementary material available at https://doi.org/10.1038/s41418-022-00958-5.

Correspondence and requests for materials should be addressed to Songbo Xie or Jun Zhou.

Reprints and permission information is available at http://www.nature.com/reprints

Publisher's note Springer Nature remains neutral with regard to jurisdictional claims in published maps and institutional affiliations.